Exploring cesium properties internal to the LANSCE H- ion source using resonant absorption spectroscopy

Kleinjan, David William
Rouleau, Gary
Neukirch, Levi Patrick

To be published in: Journal of Instrumentation

DOI to publisher's version: 10.1088/1748-0221/18/06/C06005

Exploring cesium properties internal to the LANSCE H^- ion source using resonant absorption spectroscopy

Jinst

Published by IOP Publishing for Sissa Medialab

Received: *December 22, 2022*
Accepted: *May 8, 2023*
Published: *June 7, 2023*

8th International Symposium on Negative Ions, Beams and Sources
Orto Botanico, Padova, Italy
2–7 October 2022

2023 JINST 18 C06005

Exploring cesium properties internal to the LANSCE H^- ion source using resonant absorption spectroscopy

D. Kleinjan,* L. Neukirch and G. Rouleau

Los Alamos National Laboratory,
Ls Alamos, NM, U.S.A.

E-mail: kleinjan@lanl.gov

Abstract: The Los Alamos Neutron Science Center (LANSCE) H^- ion source has provided stable output for decades of LANL mission needs, but its maximum beam output has remained the same at ~15 mA. A roadblock to improving beam output has been a lack of thorough understanding of the internal mechanisms of LANSCE H^- ion source. The LANSCE *H^- Ion Source Laser Diagnostic Stand* (HLDS) was recently built and commissioned to explore these internal mechanisms using laser absorption techniques, to measure and diagnose dynamic H^- and cesium densities. The cesium density probe is based on resonant absorption of a continuous wave diode laser tuned though the D_2 line of cesium (~852 nm). The diagnostic capabilities of HLDS will be reviewed, and measurements using the cesium laser diagnostic will be presented.

Keywords: Ion sources (positive ions, negative ions, electron cyclotron resonance (ECR), electron beam (EBIS)); Plasma diagnostics - interferometry, spectroscopy and imaging; Beam-line instrumentation (beam position and profile monitors, beam-intensity monitors, bunch length monitors)

*Corresponding author.

https://doi.org/10.1088/1748-0221/18/06/C06005

Contents

2023 JINST 18 C06005

1 Motivation

The Los Alamos Neutron Science Center (LANSCE) accelerates H^- ions to 800 MeV [1]. The LANSCE H^- Ion Source (LHIS) is a filament arc-plasma driven cesiated surface-conversion source [2]. The negative ions created at the converter surface that leave LHIS are then extracted and accelerated with the LANSCE −80 kV DC accelerating column [3], which consists of four electrodes charges sequentially from −80 kV to 0 kV. It delivers a 120 Hz, 10% Duty Factor (833 µs), 14–16 mA pulse of H^- ions.

A side view of LHIS with explanation is shown in figure 1. While a good understanding of the relationship between cesium and H^- beams inside LHIS is understood operationally using external downstream beam monitors, the internal dynamic interplay (scales of 10–1000 µs) between the plasma and caesium, and subsequent H^- formation is not extensively understood. In the case of cesium, while being the vital ingredient to make H^- beam via surface-conversion due to the resultant low work function [4], its low ionization energy can lead instabilities in LHIS operation due to large arc and/or converter current transients [5]. These instabilities can further lead to arc-downs of the −80 kV DC accelerating column, subsequently created unstable beam for LANSCE users. For H^- beam, the formation, propagation, and destruction of H^- ions internal to H^- ion sources is well debated in the field of negative ion sources [4, 6–9]. A quantification of H^- beam internal to the LHIS enviornment could help disentangle these effects, leading to improvements in overall LHIS performance, as well as provide insight for H^- formation to the global negative ion source community.

1.1 The LANSCE H⁻ Laser Diagnostic Stand

Techniques developed for fusion H^- ion sources using Tuneable Diode Laser Absorption Spectroscopy (TDLAS) to measure cesium properties (density and temperature) [10, 11], and Cavity Ring-Down Spectroscopy (CRDS) to measure the volume-averaged H- density along a line-of-sight [12], can be used to disentangle these internal dynamics. A dedicated LANSCE *H^- Ion Source Laser Diagnostic Stand* (HLDS) was developed to incorporate these measurements. An optical port was added to a

standard LHIS halfway between the converter and beam aperture, such that the laser line of sight is transverse to H^- beam and just above the Cs-reservoir transfer tube, see figure 1. Through this optical port cesium properties and H^- beam density can be measured in the heart of LHIS using TDLAS and CRDS techniques, respectively.

This paper focuses on several properties of cesium that were measured using TDLAS and will be discussed in the next section.

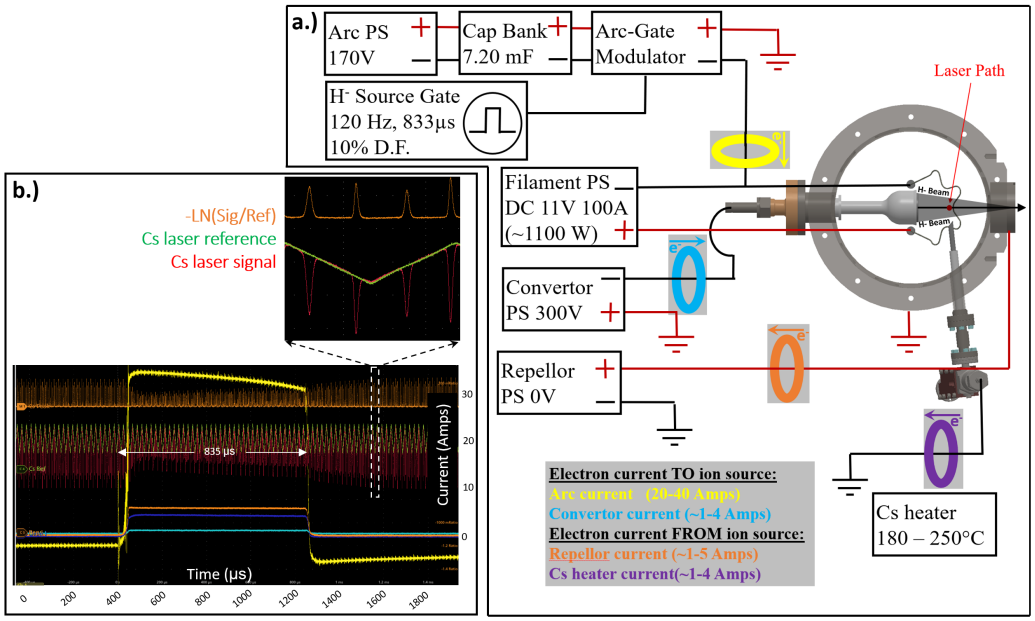

Figure 1. a.) A side-view diagram describing how LHIS works. Two tungsten filaments with 1100 W DC power are pulsed at 170 V, 120 Hz, 10% D.F. to produce a 30 amp arc pulse (yellow current monitor) that ionizes ~100 mPa of background H_2 to create a plasma. Some of this arc is grounded through the Cs-heater/reservoir transfer tube (purple current monitor) and repeller (orange current monitor). The Cs-reservoir is heated to evaporate cesium via the transfer tube onto negatively biased converter, such that H^- surface-conversion can occur with H^+, H^{2+}, H^0 from the plasma. During the arc pulse, the converter (blue current monitor) measures ~2 Amps of current, part of which is H^- dejected from the converter surface. A 48 kHz lazing signals from the TDLAS laser that sweeps through the Cs D_2 resonant line (~852.1 nm) is sent through a transverse laser path located above the Cs transfer tube and just downstream of the converter (red dot). b.) An oscilloscope trace of the measured LHIS current monitors (lower traces, described above), and qualitative laser signals (upper traces, zoomed sub-figure): a laser reference (green trace) and the LHIS line-of-sight cesium absorption signal (red trace) are divided to produce resonant absorption peaks (orange trace, upper) that can be analyzed to study cesium properties inside LHIS.

2 Cesium measurements using TDLAS

Using TDLAS set to the Cs D_2 resonant lines [13], several measurements of the LHIS cesium properties were taken. A plot of these background corrected Cs D_2 resonant lines measured in LHIS is shown in figure 2. The two resonant absorption peaks result from the electron hyperfine splitting. The gaussian shape of each peak is due to the doppler broadening of the three nuclear hyperfine states in each peak.

2023 JINST 18 C06005

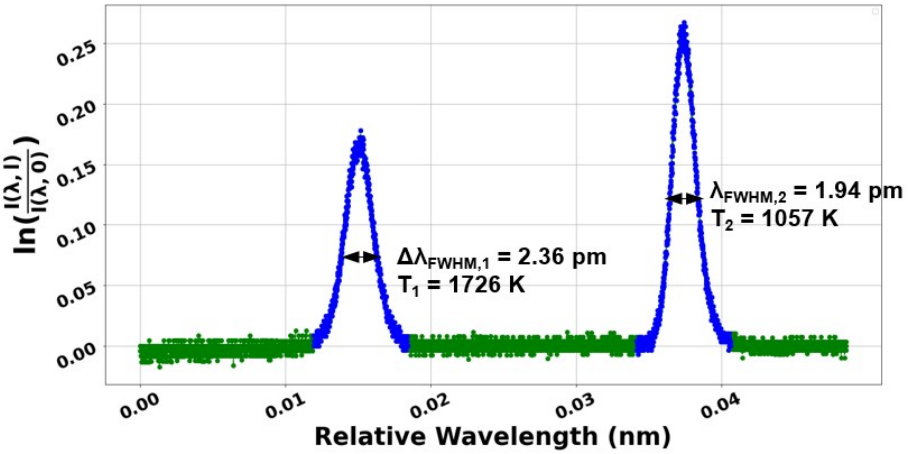

Figure 2. The background corrected D_2 resonant absorption peaks detected inside LHIS during nominal operation, just before an arc pulse. The area under the peaks can be used to calculate the cesium density [14]. The full-width-half-maximum can be used to calculate the cesium atomic temperature [10]. The difference in temperature between the two peaks is most likely due to the non-linearity of the time-to-wavelength transformation of the measurement. The average temperature $\langle T_{1,2} \rangle$ is discussed in section 2.2.

Some correction factors were considered and determined to be negligeable. Zeeman effect broadening could be ignored from the wall magnets ($\sim$ 1 kG) by both experiment and calculation. Collisional and natural broadening were ignored since the operational pressure is less than 10 Pa, and temperature is greater than 300 K [15]. No line saturation was observed during nominal operations, although some were observed during LHIS transients (see section 2.4).

Effects from depopulation of states [16] must be considered in interpreting any cesium measurements. Since neutral density filters were not used to attenuate the signal, absolute values of cesium density and atomic temperature represent an optimistic first estimate. Discussion of the following results will focus primarily on relative changes between the various measurements. In addition, no correction was made due to the non-linearity of the time-to-wavelength transformation of the TDLAS measurement [10].

Four different cesium properties were studied during commissioning of the TDLAS laser:

- Dynamic cesium density (n_{Cs}) as a function of Cs-reservoir temperature before, during and after the arc pulse
- Dynamic cesium atomic temperature (T_{Cs}) before, during and after the arc pulse.
- Static cesium density measurements just before the arc pulse, while adjusting various LHIS operational parameters.
- Cesium density during large arc current transients.

The following subsections will go through these different measurements.

2.1 Dynamic cesium density during an arc pulse

Figure 3 shows the cesium density before, during (835 µs), and after an arc pulse during nominal operational parameters (see figure 1). The first observation is that the relative densities increase

2023 JINST 18 C06005

exponentially for higher cesium reservoir oven temperatures, which correlates as expected rate of change from the vapor pressure properties of cesium [17]. The overall magnitudes are 3–4 orders of magnitude lower than the vapor pressure properties of cesium, which is likely due to impurities in the source [18].

The time-ordered effects are as follows. Before the arc pulse (400 µs), there is a thermal equilibrium density due to evaporation from the LHIS internal surfaces (body wall, converter, Cs reservoir transfer tube) due the heat of the filaments, combined with evaporation from the Cs-reservoir. Once the arc pulse turns on (450 µs), the cesium density briefly decreases due to ionization from the plasma. The density then gradually increases due to higher plasma heat load that increases evaporation rates from the internal surfaces, i.e., the plasma-wall interaction [18]. After the arc pulse turns off (1300 µs), there is an instantaneous increase (1350 µs) in the cesium density due to rapid recombination of Cs+ and electrons (seen especially at 260°C), followed by a brief decrease (1400 µs) as Cs neutrals are no longer stirred up from the plasma-wall interaction. There is a slight increase again as the source returns to a thermal equilibrium state (1600–2000 µs), which rises slightly higher than the pre-pulse thermal equilibrium state due to residual plasma heat on the internal surfaces. Eventually, the density returns to the same thermal equilibrium state as before the arc pulse for reservoir temperatures (off scale, >2000 µs).

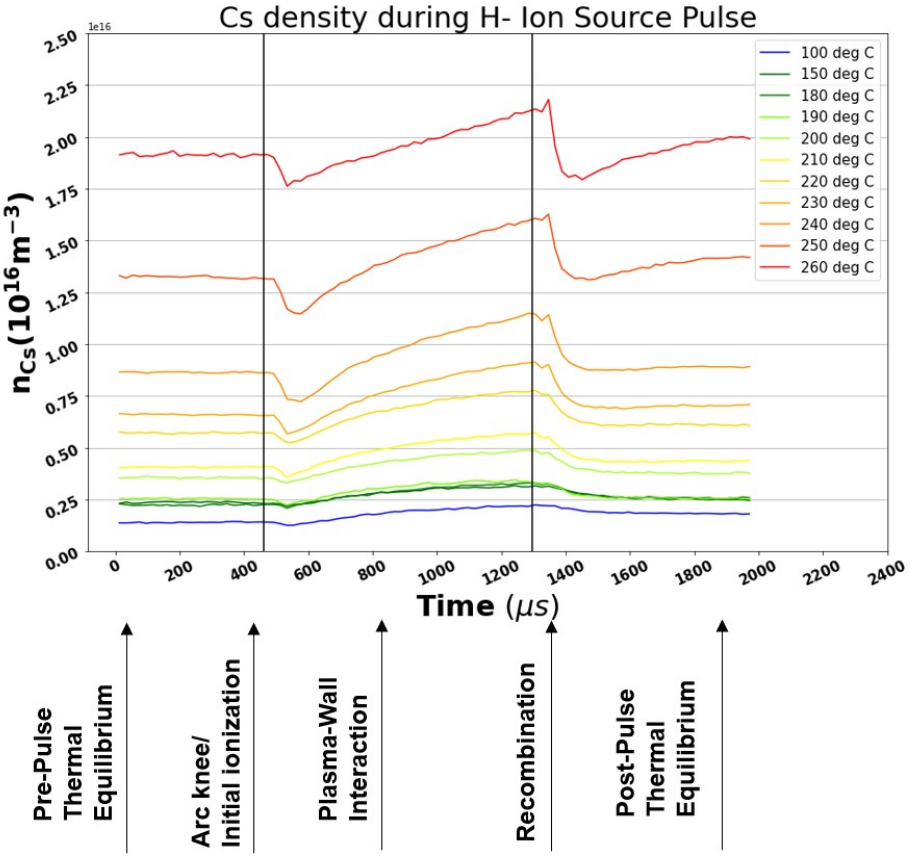

Figure 3. The cesium density (n_{Cs}) before, during and after an arc pulse. The different lines represent different Cs reservoir oven temperatures.

2023 JINST 18 C06005

2.2 Dynamic cesium atomic temperatures

Figure 4 shows the cesium atomic temperature (T_{Cs}) before, during (835 µs), and after an arc pulse during nominal operations conditions (see figure 1). The Cs reservoir temperature was set to 190°C. Temperatures were calculated using the formalism outlined in [10]. The average of the two D_2 line peaks is used as the determined temperature. The pre-pulse thermal equilibrium $T_{Cs} \sim 1200$°C, compared to the temperature ($\sim$ 1700°C) of the filaments at full power ($\sim$ 1 kW), as measured using a thermal camera [19]. Inside the plasma, $T_{Cs} \sim 4500$°C ($\sim$ 0.4 eV). To compare, the atomic temperature modelled in [20] is $T_{H+} = 0.8$ eV.

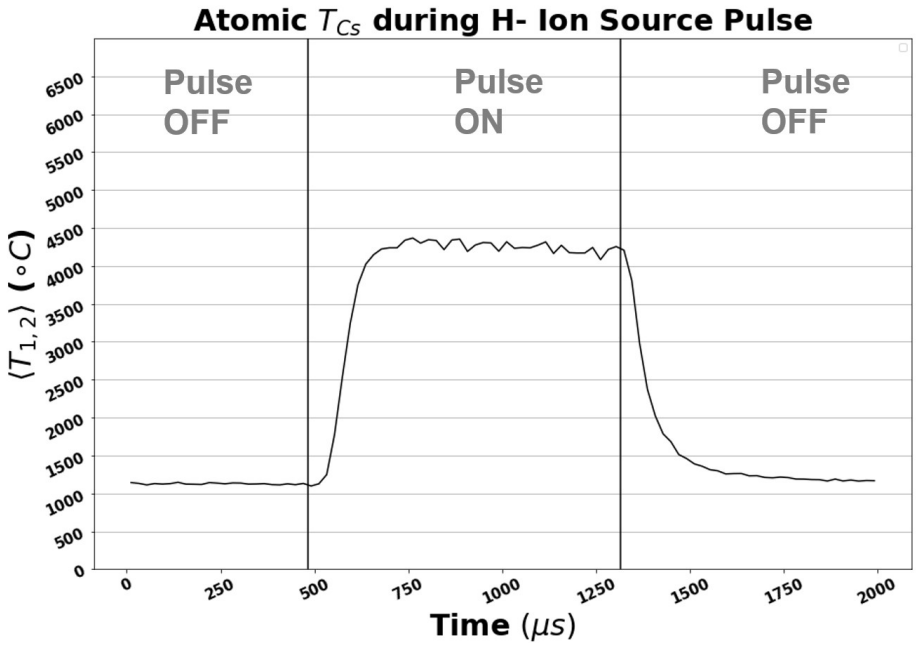

Figure 4. The atomic cesium temperature (T_{Cs}) before, during and after an arc pulse.

2.3 Static cesium density changes while adjusting different beam parameters.

For this study, LHIS was set to LANSCE operating conditions (see figure 1). A snapshot of the cesium density was recorded in the thermal equilibrium state (left part of figure 3, at $\sim$ 100 µs) while adjusting the beam parameters. The results are shown in figure 5.

These Effects shall be discussed moving from left to right in figure 5:

- We can see that the first effect is that increasing/decreasing the H_2 flow in LHIS increases/decreases the cesium density. This increase in hydrogen gas flow corresponds to increased background pressure that facilitates convective heat transfer from the filaments to evaporate cesium from the walls/converter/port.
- The next effect observed (done simultaneously while adjusting the H_2) is that increasing (decreasing) the DC power on the filaments increased (decreases) the cesium density. This is due to increased (decreased) evaporation from walls due to increased (decreased) baseline heating from the filaments.

- The power and H_2 gas flow adjustments were repeated, while also reducing LHIS water cooling temperature, specifically from 25°C to 10°C. This led to an overall decrease in the cesium density while adjusting the previous two parameters, since the reduced LHIS water cooling temperature translated to cooler internal surfaces. These cooler internal surfaces counteract the evaporative effects from the filaments/H_2.

- The final check was to adjust the power, H_2, and water cooling, while turning on/off the arc pulse, which effectively turns on and off the plasma. Once the arc pulse was on, adjusting the previous mentioned parameters had little effect, and the cesium density settled into an equilibrium state. This is likely due to the fact that the plasma also redistributes cesium between the converter and walls at a much higher rate than the evaporative effects of the filaments alone, thus the plasma dominates the behavior when both are present. This indicates the necessity of a continual background cesium transfer to maintain an optimal cesium layer on the converter for LHIS H^- beam production during continuous LHIS pulsing.

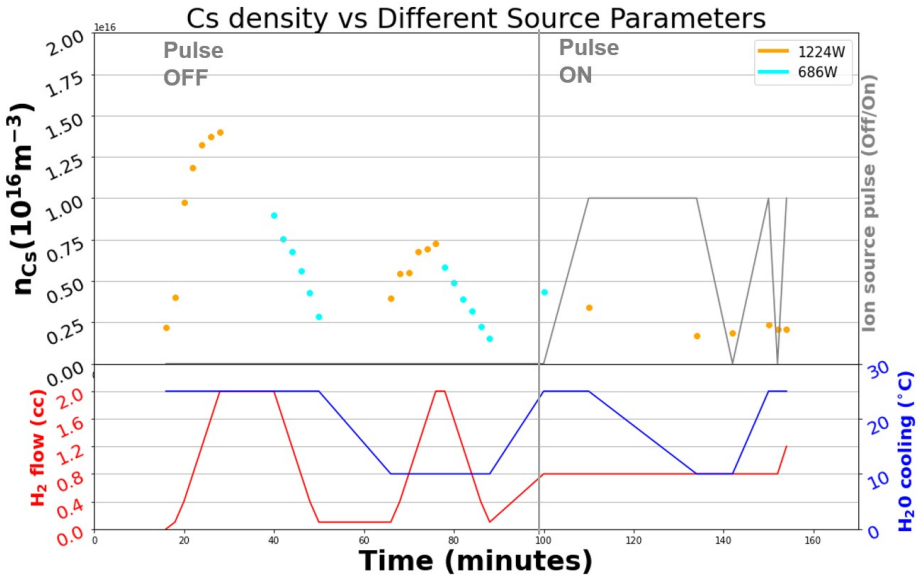

Figure 5. The Cs density recorded vs changes in various LHIS operational parameters. The parameters adjusted are the filament power, H_2 gas flow, water cooling, and turning the pulser on and off.

2.4 Cesium density during a LHIS current transient instability

Recently, attention has been given to large arc and/or converter current transients (~300 Amps) on random arc pulses inside LHIS [5]. Depending on the cesium conditions, they can occur anywhere from once a day to several per minute. Part of this excess electron load from these transients leaves the ion source and gets extracted by the LANSCE 80 kV extraction column. This excess load can lead to arc downs of the column, which subsequently leads to instability in delivered H^- beam to the LANSCE user facilities.

While it has been understood that cesium plays a central role in these transients, it is unclear how the transient is initiated. One hypothesis is a "cesiated plasma effect". Since cesium in the

2023 JINST 18 C06005

plasma reduces the voltage required to produce an arc pulse, a random, localized high density of cesium that develops in the dynamic plasma environment can cause the filament and/or converter to short through the cesiated plasma to surrounding surfaces, producing a transient. Another hypothesis is the "non-uniform cesium deposit effect" on the internal surfaces that develop over time during LHIS operations or from a "cesium burst" from the Cs-reservoir transfer tube. These deposits evaporate/sputter non-uniformly from an otherwise uniform cesium evaporation. They can lead to localized "Paschen pockets" [21] that create a path to ground for the filament arc and/or converter currents. A demonstration of the latter hypothesis given in figure 6.

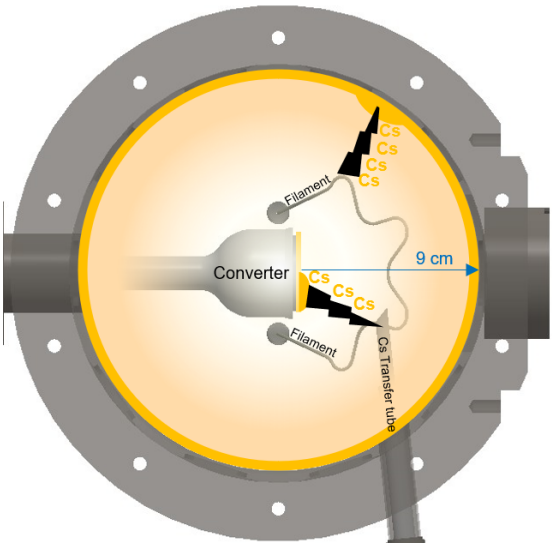

Figure 6. A side-view demonstration of the cesium distribution inside the ion source. Nominally, a uniform coating exists on the walls and the converter, which leads to a uniform cesium evaporation into the ion source. Sporadic development of non-uniform cesium deposits on the walls and/or converter may lead to LHIS instabilities via arc and converter current transients.Nominally, a uniform coating exists on the walls and the converter, which leads to a uniform cesium evaporation into the ion source. Sporadic development of non-uniform cesium deposits on the walls and/or converter may lead to LHIS instabilities via arc and converter current transients.

Figure 7 shows an oscilloscope trace where transients were observed on HLDS. A sequential description of the plot is given.

1.) Nominal arc pulses occur.

2.) The 1st transient. The arc current (yellow trace) and the converter (blue trace) current saturate. Once the arc pulse turns off, the relative cesium signal considerably increases.

3.) A 2nd transient.

4.) The cesium density in the line-of-sight of the TDLAS signal is intense enough after the 2nd transient to cause line saturation.

5.) Another arc current transient, but much smaller.

6.) Arc pulses slowly return to nominal state.

2023 JINST 18 C06005

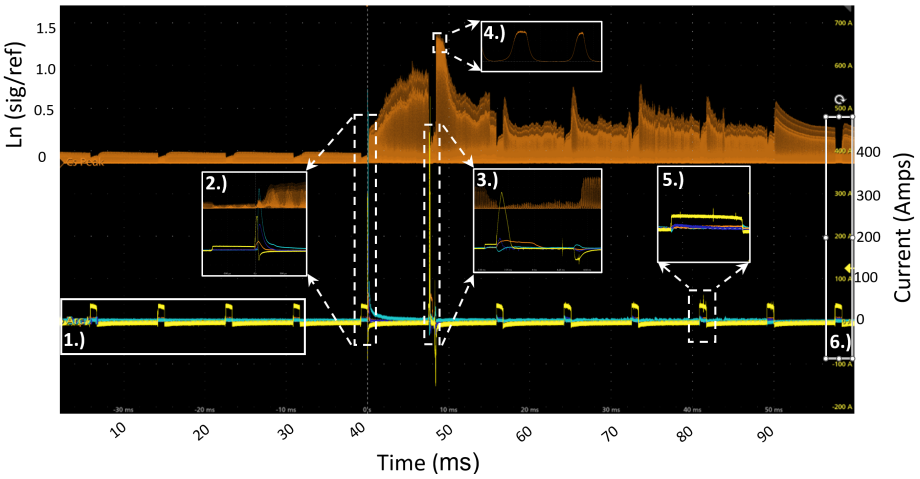

Figure 7. A LHIS instability due to arc and converter transients as detected on HLDS. The color scheme is the same as figure 1. The plot displays multiple LHIS arc pulses. Events 1–6.) are described in the text. Note that 2–5.) are zoomed in sub-figures of the dashed boxes.

The most important observation is that there is no observed anomaly in the relative cesium density before the 1st transient takes place. This essentially eliminates the cesiated plasma effect since the line-of-sight path of the laser should detect these as dynamic changes to the cesium density just before the transient. The fact that the density increases after the arc pulse hints that the filament arc current is spiking via the non-uniform deposit effect. This deposit is instantaneously highly thermalized and leads to massive density detection after the transient.

3 Conclusions

From the first commissioning run of the HLDS, we were able to get initial dynamic measurements of the cesium density and cesium atomic temperature inside the H^- Ion source during nominal operations using TDLAS. Changes to cesium density were observed for adjusting various ion source operational parameters. Observing the timing and change in magnitude of the resonant absorption peaks during LHIS transient give evidence that non-uniform cesium build-ups in the ion source are the predicted cause of these transients.

HLDS has also been commissioned to take H^- density data using CRDS, and H^- density will be taken during the next HLDS experimental run. Additionally, future upgrades to HLDS are being planned, such as adding a high-voltage extraction and H^- beam current monitor.

Acknowledgments

We are grateful and acknowledge our collaborators at the Max Planck Institute for Plasma Physics in Garching, Germany for this work, with special thanks to U. Fantz, D. Wunderlich, C. Wimmer, and A. Mimo. We acknowledge LANL colleague Anna Alexander for review of this work. We also thank and acknowledge our funding sources: the LANL LDRD program, the US DOE, and NNSA.

2023 JINST 18 C06005

References

[1] R.W. Garnett, *LANSCE Accelerator Update and Future Plans*, *J. Phys. Conf. Ser.* **1021** (2018) 012001.

[2] R. Keller et al., *H^- Ion Source Development for the LANSCE Accelerator Systems*, *AIP Conf. Proc.* **1097** (2009) 161.

[3] J. Bradley III et al., *Test Results of the Low-Stored-Energy −80 kV Regulator for Ion Sources at LANSCE*, in the proceedings of the *10th International Particle Accelerator Conference*, Melbourne, Australia (2019), p. TUPMP053 [DOI:10.18429/JACoW-IPAC2019-TUPMP053].

[4] B. Rasser, J. Van Wunnik and J. Los, *Theoretical models of the negative ionization of hydrogen on clean tungsten, cesiated tungsten and cesium surfaces at low energies*, *Surf. Sci.* **118** (1982) 697.

[5] D. Kleinjan, *Arc and Convertor Transient Studies for Multi-cusp Cesiated Surface-Conversion H- Source at LANSCE*, in the proceedings of the *10th International Particle Accelerator Conference*, Melbourne, Australia (2019).

[6] J.R. Hiskes, *Formation of hydrogen negative ions by surface and volume processes with application to negative ion sources*, *J. Phys. Colloques* **40** (1979) C7-179.

[7] M. Seidl, H.L. Cui, J.D. Isenberg, H.J. Kwon, B.S. Lee and S.T. Melnychuk, *Negative surface ionization of hydrogen atoms and molecules*, *J. Appl. Phys.* **79** (1996) 2896.

[8] T. Okuyama and Y. Mori, *Cesium catalyzed effect of H- ion production in volume production type of H- ion source*, *Rev. Sci. Instrum.* **63** (1992) 2711.

[9] R. McAdams and M. Bacal, *The negative ion flux across a double sheath at the formation of a virtual cathode*, *Plasma Sources Sci. Technol.* **19** (2010) 042001.

[10] M. Lindaur, *Investigation of the caesium dynamics using TDLAS at the large-scale negative hydrogen ion source of ELISE*, MSc Thesis, Universität Augsburg (2017).

[11] U. Fantz and C. Wimmer, *Optimizing the laser absorption technique for quantification of caesium densities in negative hydrogen ion sources*, *J. Phys. D* **44** (2011) 335202.

[12] A. Mimo, H. Nakano, C. Wimmer, D. Wünderlich, U. Fantz and K. Tsumori, *Cavity ring-down spectroscopy system for the evaluation of negative hydrogen ion density at the ELISE test facility*, *Rev. Sci. Instrum.* **91** (2020) 013510.

[13] A. Steck, *Cesium D line data*, available online at http://steck.us/alkalidata, revision 2.1.4, 23 December 2010 (2010).

[14] A.J.M. Buuron, D.K. Otorbaev, M.C.M. van de Sanden and D.C. Schram, *A new absorption spectroscopy setup for the sensitive monitoring of atomic and molecular densities*, *Rev. Sci. Instrum.* **66** (1995) 968.

[15] R. Feidl, *Experimental investigations on the caesium dynamics in H2/D2 low temperature plasmas*, MSc Thesis, Universität Augsburg (2013).

[16] E.U. Condon, *Intensity-Dependent Absorption of Light*, *Proc. Nat. Acad. Sci.* **52** (1964) 635.

[17] Y. Ralchenko, A. Kramida, R.J. and N.A. Team, *2010 NIST Atomic Spectra Database (ver. 4.0.1)*, available online at http://physics.nist.gov/asd [29 December 2010].

[18] U. Fantz and A. Mimo, private communication, Max Planck IPP (2020).

[19] G. Rouleau, private communication, Los Alamos National Laboraotry.

[20] M. Bacal, R. McAdams and B. Lepetit, *The negative ion mean free path and its possible implications*, *AIP Conf. Proc.* **1390** (2011) 13.

[21] M. Stokli, *RF (Light) Negative Ion Sources for Non-Fusion Applications, a tutorial*, presentation at *8th International Symposium on Negative Ions, Beams and Sources*, Orto Botanico, Padova, Italy, 2–7 October 2022.

2023 JINST 18 C06005